

G-2-3

Nondestructive characterization of temperature-dependent backbone Si-O-Si structure in porous silica films by *in-situ* Fourier-transform infrared spectroscopy

Syozo Takada¹, Nobuhiro Hata^{1,2}, Xianying Li¹, Nobutoshi Fujii³,
Takahiro Nakayama³, and Takamaro Kikkawa^{2,4}

¹ASRC, AIST, 16-1 Onogawa, Tsukuba, Ibaraki 305-8569, Japan E-mail: n.hata@aist.go.jp

²MIRAI-ASRC, AIST, 16-1 Onogawa, Tsukuba, Ibaraki 305-8569, Japan

³MIRAI-ASET, 16-1 Onogawa, Tsukuba, Ibaraki 305-8569, Japan

⁴RCNS, Hiroshima University, 1-4-2 Kagamiyama, Higashi-Hiroshima 739-8527, Japan

1. Introduction

Interconnect structures including interlayer low-dielectric-constant (low-k) films experience thermal cycles between room temperature to elevated process temperatures during back-end-of-line process integration, so that the structure and properties of the component materials such as porous low-k films at the elevated temperatures are of great concern to clarify possible origins of process-induced damages. We have reported that room-temperature Fourier transform infrared (FTIR) spectroscopy is a powerful nondestructive characterization technique for chemical bonding features of *skeletal* backbone in porous low-*k* films, and that FTIR spectral features originating from the *skeletal* Si-O-Si bonds in porous silica films correlate with their *skeletal* mechanical strength [1, 2]. In the present work, we employ the FTIR analysis technique for porous silica films to reveal the backbone Si-O-Si structure at an elevated temperature.

2. Experimental

Two types of porous silica films, sample A and B, were prepared on Si by spin-coating of a precursor solution of acidic silica sol with cationic cetyltrimethylammonium chloride [3] and nonionic surfactant [4] templates, respectively. Properties of the samples are listed in Table I.

A closed sample chamber with two infrared windows was employed to measure FTIR transmission spectra *in-situ* in dry N₂ flow at elevated sample temperatures. Measurements of the substrate Si only at the temperatures were also carried out to subtract the contributions from the substrate to the obtained spectra. Regression analysis of the spectra with an optical model in which multiple reflection within single-layer porous silica film on Si was employed to obtain infrared complex dielectric function [5]. A dispersion model with multiple Lorenz oscillators was used in the analysis, while the film thickness and refractive index were fixed at the values obtained from UV-visible spectroscopic ellipsometry of the same samples.

3. Results and Discussion

Figure 1 shows the infrared-absorbance spectra, measured at 20, 100, 150, 200, 250 °C, of sample A. The broad peak which appears at 3500 cm⁻¹ and the sharp peak at 3740 cm⁻¹ are assigned as the O-H stretching vibrations of adsorbed H₂O and silanol groups, respectively. The

adsorbed H₂O peak intensity decreases with the temperature as is seen in Fig. 1, while the silanol peak intensity stays constant. We experimentally observed that the amount of adsorbed H₂O does affect the infrared spectral peak in between 1000-1400 cm⁻¹, which is assigned as the asymmetric stretching mode of skeletal Si-O-Si network. Differential scanning calorimetry (DSC) result from the same sample is shown as the inset of Fig. 1, in which the endothermic peak appearing at 100°C corresponds to the H₂O desorption from the porous silica film. Further experiments were carried out after drying the samples to avoid the effects of the adsorbed H₂O.

Figure 2 shows the infrared absorbance spectra measured at 20 and 283 °C of the *dry* sample A. The observed spectral dependence on temperature was confirmed to be reversible. The inset of Fig. 2 shows the DSC result, which evidences the absence of the adsorbed H₂O in the *dry* sample A. Figure 3 shows the infrared complex dielectric function of skeletal backbone of the porous silica sample A. Bruggeman's effective medium approximation was employed to take into account the effect of pores onto the apparent spectrum [2]. The Si-O-Si peak got shifted to lower wavenumber with the measurement temperature. The bridging angles θ of Si-O-Si were calculated from the peak position ν of imaginary parts of infrared complex dielectric function, using the central and non-central force network model [6], which is expressed as

$$\nu = [2(\alpha \sin^2(\theta/2) + \beta \cos^2(\theta/2))/m_o]^{1/2} / 2\pi c \dots (1)$$

where m_o , α , β , θ , and c are the mass of O atom, central and non-central force constants, bridging angle of Si-O-Si and the speed of light, respectively. Figure 4 shows θ calculated by eq. (1) from the results in Fig. 3. Here, α and β were assumed as 620 and 100 N m⁻¹, respectively [6]. The bond angle θ shifted to lower direction with the measurement temperature as much as 2.9 %. The similar temperature dependencies of infrared complex dielectric function and bond angle distribution were observed for sample B, as shown in Figs. 5 and 6, respectively.

4. Conclusions

We have reported a nondestructive structural characterization at an elevated temperature of skeletal Si-O-Si bond angle θ of porous silica low-k films. θ shifted to lower wavenumber by 2.9 % from 20 to 283 °C.

Acknowledgements

Japan Science and Technology Agency (JST) is acknowledged for Cooperative System for Supporting Priority Research. This work was partly supported by New Energy Development and Industrial Technology Organization (NEDO).

References

- [1] S. Takada, *et al.*, Jpn. J. Appl. Phys. **43** (2004) 2455.
- [2] S. Takada, *et al.*, J. Appl. Phys. **97** (2005) 113504.
- [3] D. Kundu, *et al.*, J. Mat. Sci. Lett. **17** (1998) 2089.

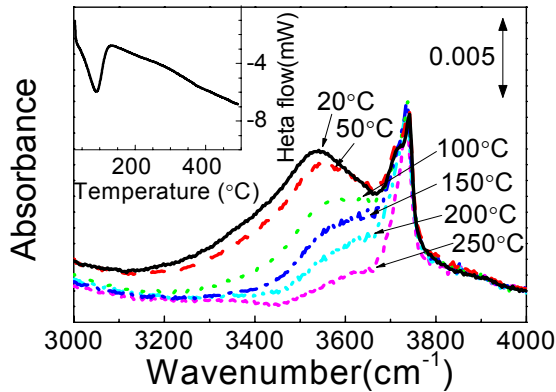


Fig. 1 Infrared absorbance spectra of porous silica sample A at the six different measurement temperatures. Inset is a DSC curve of the as prepared sample.

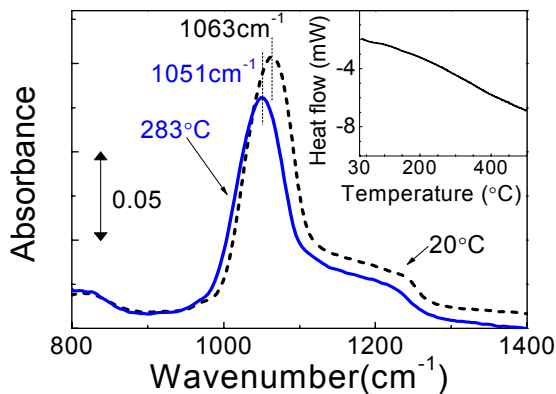


Fig. 2 Infrared absorbance spectra of the *dry* sample A measured at 20 and 286 °C. Inset is a DSC curve.

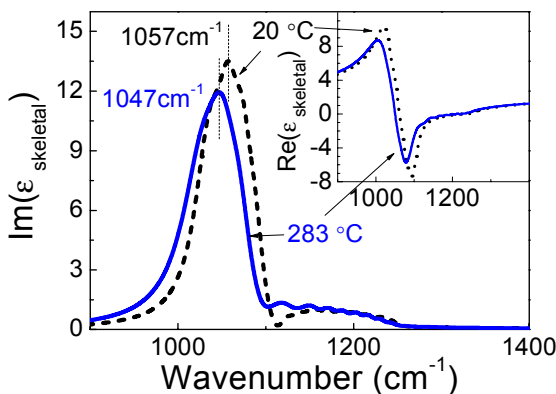


Fig. 3 Real and imaginary parts of mid-infrared complex dielectric function of porous silica skeleton of the sample A.

- [4] N. Fujii, *et al.*, Mat. Res Soc. Symp. Proc. **812** (2004) 43.
- [5] S. Takada, *et al.*, Ext. Abs. SSDM 2005, p.552.
- [6] K. Ishikawa, *et al.*, J. Appl. Phys. **88** (2000) 7150.

Table I Properties of sample A and B.

Sample	t (nm)	n at 633nm	Pore structure
A	234	1.24 ₉	Periodic
B	278	1.25 ₇	Disorder

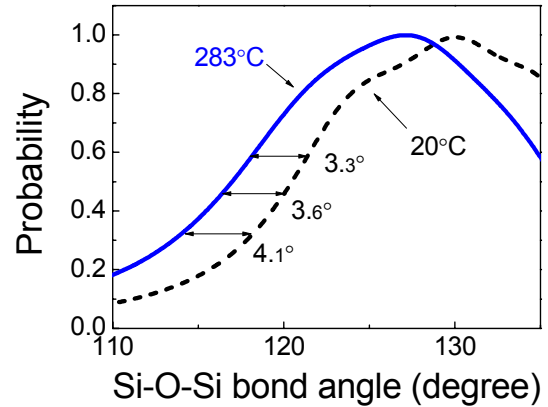


Fig. 4 The distribution of θ in sample A calculated from the results in Fig.3, with a central and non-central force network model.

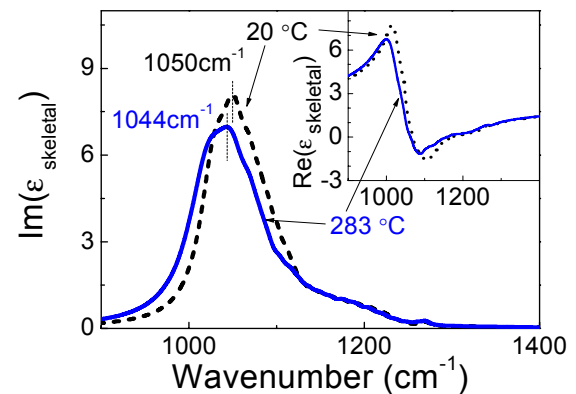


Fig. 5 Real and imaginary parts of mid-infrared complex dielectric function of sample B

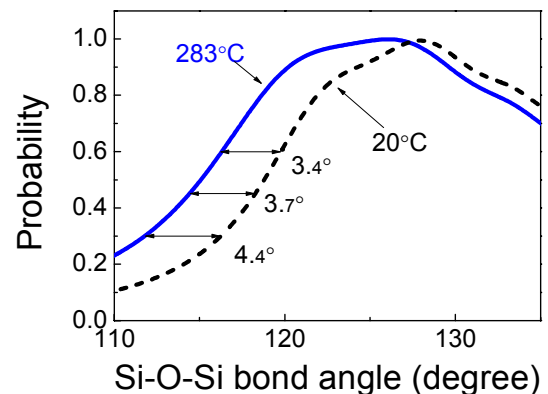


Fig. 6 The distribution of θ in sample B calculated from the results in Fig.5, with a central and non-central force network model.